

Pressure-driven orbital reorientation and change in Mott-Hubbard gap in YTiO₃

I. Loa,^{1,*} X. Wang,¹ K. Syassen,¹ H. Roth,² T. Lorenz,² M. Hanfland,³ and Y.-L. Mathis⁴

¹Max-Planck-Institut für Festkörperforschung, Heisenbergstr. 1, D-70569 Stuttgart, Germany

²Universität zu Köln, II. Physikalisches Institut, Zùlpicher Str. 77, D-50937 Köln, Germany

³European Synchrotron Radiation Facility, BP 220, F-38043 Grenoble, France

⁴ANKA/ISS, Forschungszentrum Karlsruhe, PF 3640, D-76021 Karlsruhe, Germany

(Dated: June 23, 2018)

We investigate the crystal structure of YTiO₃ at high pressures up to 30 GPa by synchrotron x-ray powder diffraction ($T = 295$ K). The variation of the Ti–O bond lengths with pressure evidences a distinct change in the distortion of the TiO₆ octahedra at around 10 GPa, indicating a pressure-driven spatial reorientation of the occupied Ti $3d(t_{2g})$ orbitals. The pressure-induced reduction of the optical band gap of YTiO₃ is determined quantitatively by mid-infrared synchrotron micro-spectroscopy and discussed in terms of bond length and orbital orientation changes.

PACS numbers: 61.50.Ks, 61.10.Nz, 71.30.+h

Orbital ordering, fluctuation and excitation phenomena of $3d$ electrons in transition metal perovskites have attracted much interest. For e_g electron systems like LaMnO₃ [electron configuration $3d^4(t_{2g}^3e_g^1)$], lifting of energetic degeneracies due to lattice distortions (Jahn-Teller effect) and concomitant spatial ordering of the occupied e_g orbitals are well known. In contrast, the t_{2g} states in systems like rare-earth titanates [configuration $3d^1(t_{2g}^1)$] have often been assumed to be degenerate and thus in disfavor of orbital ordering. YTiO₃ [Fig. 1(a)] is a prototypical Mott-Hubbard insulator with ferromagnetic ground state, where the question of t_{2g} orbital ordering has been studied in some detail. Static ordering was predicted theoretically [1, 2] and confirmed in nuclear magnetic resonance [3] and several other experiments [4, 5, 6]. The mechanism and energetics of the ordering were studied in theoretical work [7, 8, 9, 10]. In contrast to these experimental and theoretical findings, the experimentally observed spin-wave excitation spectrum was taken as evidence for strong orbital fluctuations [11, 12]. However, an alternative explanation, compatible with orbital order, has been proposed [10].

Altogether, these recent studies raise a number of questions. How robust is orbital ordering in t_{2g} electron systems like YTiO₃? Which factors determine the orbital ordering in a particular compound? Can it be tuned by external parameters such as high pressure? How does orbital order relate to other physical properties, e.g., the electronic and magnetic excitation spectra? The orbital polarizations in the rare-earth titanates manifest themselves in small distortions of the TiO₆ octahedra [9]. It is therefore possible to study the orbital ordering of YTiO₃ by structural methods.

In this letter, we demonstrate that the TiO₆ octahedra remain distorted under pressure, showing the persistence of orbital ordering. This order is, however, not an immutable property: experimental evidence is presented that the Ti $3d(t_{2g})$ orbitals undergo a *pressure-driven reorientation*. To relate the structural/orbital changes to

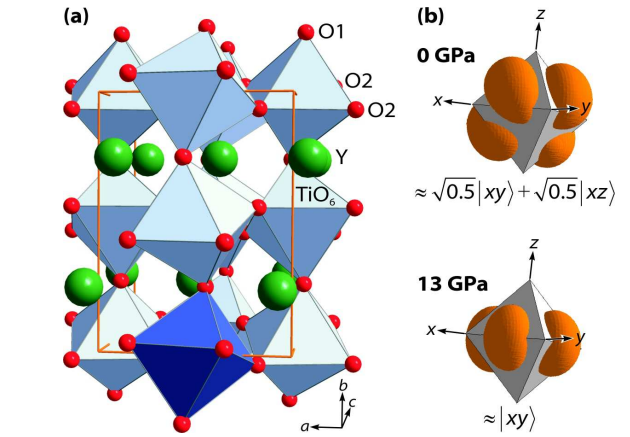


FIG. 1: (a) Perovskite-type (GdFeO₃) crystal structure of YTiO₃ (space group $Pnma$) [13]. (b) Orientation of the titanium $3d^1(t_{2g})$ wavefunction at 0 and 13 GPa as derived in this work from the TiO₆ octahedral distortion. The orbitals shown refer to the Ti site highlighted in (a). The octahedra in (b) illustrate the octahedral environment of the orbitals, but they do not match the size of the actual TiO₆ octahedra.

the electronic properties of YTiO₃, we determine quantitatively (by mid-infrared spectroscopy) how the Mott-Hubbard gap decreases under pressure.

Angle-dispersive x-ray powder diffraction experiments were performed at the beamline ID09A of the European Synchrotron Radiation Facility in Grenoble. A fine powder was produced from an YTiO₃ crystal (Curie temperature $T_C = 28$ K) grown by a floating zone technique [14]. The sample was pressurized in a diamond-anvil cell using condensed nitrogen as the pressure-transmitting medium. Two-dimensional diffraction images were recorded with an image plate detector and converted to intensity-vs- 2θ diffractograms [Fig. 2] by numerical integration [15]. The structural parameters were determined by means of Rietveld refinements [16, 17]. In contrast to the common practice, we calculated the statistical uncertainties of the diffraction intensities from the intensity variations

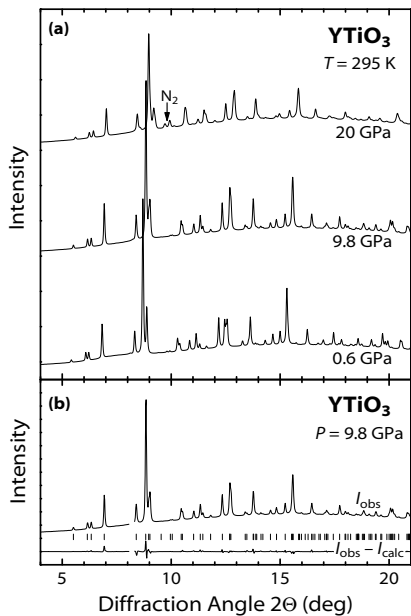


FIG. 2: (a) Selected x-ray diffraction diagrams of YTiO₃ for pressures up to 20 GPa ($T = 295$ K, $\lambda = 0.41$ Å). (b) Rietveld refinement of data recorded at 9.8 GPa. I_{obs} and I_{calc} denote observed and calculated diffraction intensities, respectively. Markers show the calculated peak positions.

along the individual diffraction rings, rather than assuming basic counting statistics ($\Delta I \propto \sqrt{I}$). Using the experimentally determined uncertainties as weights in the Rietveld fitting process turned out to be essential for an accurate determination of the oxygen atomic positions. Mid-infrared transmission experiments were conducted at the infrared beamline of the synchrotron ANKA in Karlsruhe. The spectra were recorded on 40 μm thick YTiO₃ crystals with a Bruker IFS66v/S Fourier transform spectrometer equipped with an MCT detector and a microscope using mirror objectives. Synthetic type-IIa diamond anvils were used in the infrared experiments. Condensed nitrogen and solid KCl were employed as pressure media. Pressures were determined in all experiments with the ruby luminescence method [18].

The diffraction diagrams of YTiO₃ (Fig. 2) and the measured lattice parameters [Fig. 3(a, b)] change continuously with pressure. The ambient-pressure perovskite-type crystal structure of YTiO₃ is thus stable under compression up to at least 30 GPa. The compressibility exhibits a distinct anisotropy with the a direction being only about half as compressible as the b and c directions [Fig. 3(b)]; the orthorhombic strain increases with pressure. A Birch equation of state was fitted to the pressure-volume data up to 30 GPa to determine the bulk modulus $B_0 = 163(6)$ GPa and its pressure derivative at zero pressure $B' = 8.5(10)$; the zero-pressure volume was fixed at the measured value of $V_0 = 231.78(2)$ Å³. The increasing distortion is evident also from the variation of

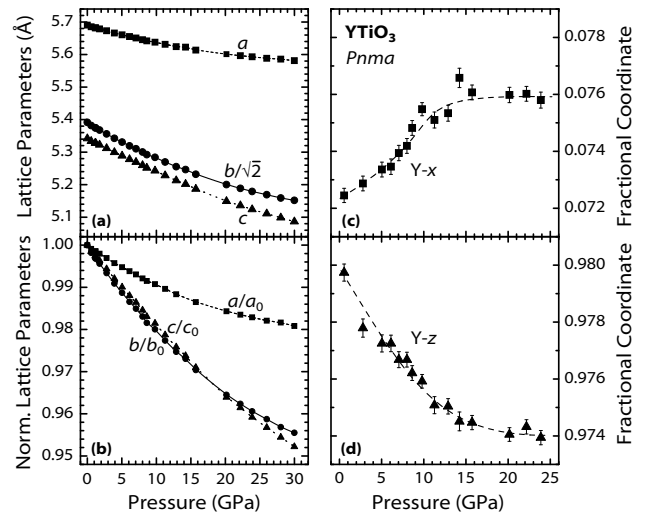


FIG. 3: Structural parameters of YTiO₃ as a function of pressure. (a) Lattice parameters, (b) lattice parameters normalized to their respective zero-pressure values, (c, d) x and z fractional coordinates of Y. The lattice parameter b was scaled by $\sqrt{2}$ in (a) to obtain a pseudo-cubic representation.

the yttrium coordinates x and z with pressure shown in Fig. 3(c, d) [$y = 1/4$ by symmetry]. Under pressure, the yttrium ions clearly move further away from the “ideal” position $(0, 1/4, 1)$ in an undistorted (cubic) perovskite. This shift levels off, however, at around 15 GPa.

The variations of the Ti–O distances with pressure (Fig. 4) represent the most important structural information. At ambient pressure, the long Ti–O2(a) distance exceeds the two shorter ones by $\sim 3\%$ [Ti–O2(a) and Ti–O2(b) denote the two distinct Ti–O2 distances]. This type of distortion persists up to about 8 GPa. When increasing the pressure further, the initially short Ti–O2(b) distance *lengthens* with increasing pressure, while Ti–O2(a) shortens markedly. As a result, the two Ti–O2 bond lengths become (i) nearly equal at 13 GPa and (ii) distinctly larger than the Ti–O1 distance.

As has been described in detail before [4, 9], the deformation of the TiO₆ octahedra reflects the spatial orientation of the t_{2g} wavefunction. To facilitate the discussion, we introduce a *local* coordinate system at each Ti site with the x , y , and z axes parallel to the Ti–O2(a), Ti–O2(b), and Ti–O1 bonds, respectively [Fig. 1]. The relative Ti–O distances at 0 GPa (long along x ; short along y and z) indicate nearly equal occupancy of the $|xy\rangle$ and $|xz\rangle$ orbitals. Thus, the eigenfunction is $\approx \sqrt{0.5}|xy\rangle + \sqrt{0.5}|xz\rangle$, in agreement with the experimental results [3, 4, 5, 6] and theoretical studies [1, 2, 7, 8, 9].

At 13 GPa, the TiO₆ octahedra are characterized by two equally long Ti–O2 bonds along x , y and a shorter Ti–O1 distance along z , i. e., the octahedra are compressed along z . Such a distortion indicates predominant occupation of the $|xy\rangle$ orbital. In fact, the relative Ti–O bond lengths in YTiO₃ above 13 GPa are very similar

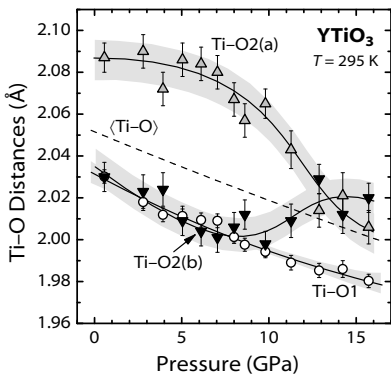


FIG. 4: Ti-O bond lengths in YTiO_3 as a function of pressure (symbols). $\langle \text{Ti-O} \rangle$ denotes the average bond length (dashed line). Grey bands indicate estimated confidence bands; solid lines are guides to the eye.

to those in SmTiO_3 at ambient pressure, where there is theoretical support for a predominant occupation of the $|xy\rangle$ orbitals [9]. The changes in the Ti-O bond lengths observed in YTiO_3 thus provide evidence of a pressure-induced reorientation of the t_{2g} orbitals from the initial “tilted state” with the approximate wavefunction $\sqrt{0.5}|xy\rangle + \sqrt{0.5}|xz\rangle$ to a situation where essentially only the $|xy\rangle$ orbital is occupied, as shown in Fig. 1(b).

It is interesting to note that the orbital reorientation does not correlate with anomalies in the average Ti-O distance [Fig. 4], the lattice parameters [Fig. 3(a, b)], or the Ti-O-Ti bond angles [Fig. 5]. In contrast, the change in the pressure-induced shift of the Y ions at 10–15 GPa [Fig. 3(c, d)] coincides with the Ti t_{2g} orbital reorientation.

For a qualitative discussion of the origin of the orbital reorientation under pressure, we consider the results of recent theoretical investigations [9, 10]. Essentially, one has to take into account two effects that induce a splitting of the t_{2g} states. Firstly, in the presence of the GdFeO_3 -type distortion, the crystal field of the Y ions lifts the degeneracy of the Ti t_{2g} states. This splitting will increase if the Y-Ti distances are shortened, i.e., under pressure. Secondly, a Jahn-Teller distortion due to the Ti-O interaction can modify or even dominate the energetics of the Ti t_{2g} states. Due to the stiffening of the lattice, Jahn-Teller distortions will usually become less favorable under compression [19]. Application of high pressure is thus expected to tune the balance between these two contributions. In terms of relative Ti-O bond lengths, the situation in YTiO_3 at 15 GPa is quite similar to that in SmTiO_3 at ambient pressure. In the latter case, there exists no Jahn-Teller distortion of the type encountered in YTiO_3 , and the competition between the crystal field of the rare-earth ions and that of the O ions was reported to be rather balanced [20]. Quite likely, this scenario applies also to YTiO_3 at ~ 15 GPa.

The similarity between YTiO_3 and SmTiO_3 has im-

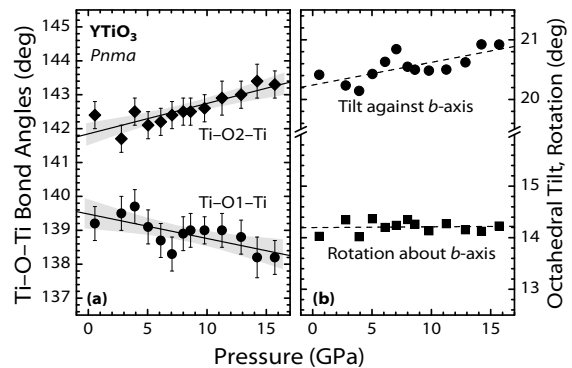


FIG. 5: (a) Ti-O-Ti bond angles and (b) octahedral tilt and rotation angles in YTiO_3 as a function of pressure. Lines are guides to the eye; the shaded bands indicate confidence bands.

portant implications regarding magnetism. In contrast to YTiO_3 , SmTiO_3 is an antiferromagnet [21]. In view of the orbital reorientation and the coupling between spins and orbitals, one may speculate that YTiO_3 becomes antiferromagnetic under pressure. YTiO_3 would then lose its unusual property of being simultaneously ferromagnetic and insulating. More generally, application of pressure to YTiO_3 may cause similar changes in the electronic and magnetic properties as a substitution of Y by larger rare-earth ions.

We turn now to the question of the electronic excitation spectrum of YTiO_3 under pressure and whether it is affected by the orbital reorientation. Figure 6 depicts spectra of the reciprocal transmittance $1/T$ [which is related to the absorbance $A = \log_{10}(1/T)$] for several pressures up to 16 GPa. In this representation, the optical absorption edge and its pressure-induced red shift are easily recognized. To obtain quantitative results on the red shift, we determine the energies where $1/T = 300$ (corresponding to an optical conductivity of $\sim 10 \text{ } \Omega^{-1} \text{ cm}^{-1}$). The ambient-pressure optical gap thus determined at the onset of absorption amounts to $\sim 5300 \text{ cm}^{-1}$ (0.7 eV), a number that is naturally somewhat smaller than the previously reported values of 6500–8000 cm^{-1} (0.8–1.0 eV) deduced from reflectance measurements [22, 23]. The important information here is the shift of the absorption edge [Fig. 6(b)] rather than its absolute value. In the higher-pressure range, the optical band gap decreases essentially linearly with pressure at a rate of $-145(10) \text{ cm}^{-1}/\text{GPa}$. On the basis of a linear extrapolation of these data, the optical gap is expected to close at a pressure in the order of 40 GPa.

The mid-IR optical absorption of rare-earth titanates has been attributed to an excitation across the Mott-Hubbard gap [22, 24]. The Coulomb repulsion U is not expected to change under pressure so that the reduction in bandgap is a measure of the increase in bandwidth. The increasing electronic bandwidth under pressure is usually interpreted in terms of the Ti-O bond lengths

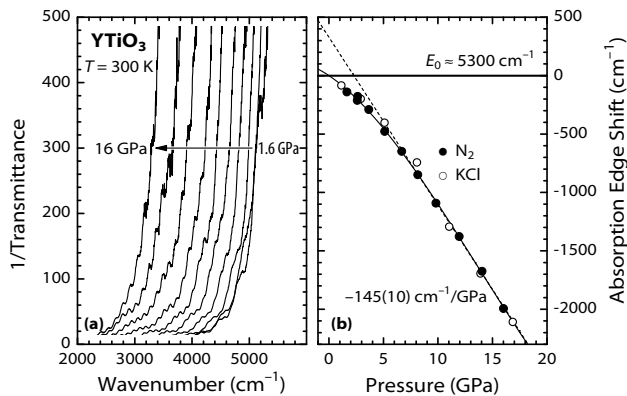


FIG. 6: Mid-infrared optical absorption in YTiO_3 under pressure ($T = 295$ K). (a) $1/\text{Transmittance}$ spectra recorded at pressures of 1.6, 2.6, 3.7, 5.1, 6.7, 8.2, 9.8, 12.0, 14.1, and 16.0 GPa (with nitrogen pressure medium). The modulations of the spectra originate from interferences. (b) Pressure-induced shift of the optical absorption edge determined at $1/\text{Transmittance} = 300$ from two experimental runs with condensed nitrogen and KCl pressure medium, respectively.

and the Ti–O–Ti bond angles. In the present case, the changes in the bond angles, i.e. $\pm 1^\circ$ up to 16 GPa, are relatively small compared to related perovskites like rare-earth nickelates [25] or LaMnO_3 [19]. In fact, the *average* bond angle is essentially pressure-insensitive due to the opposite changes of Ti–O1–Ti and Ti–O2–Ti. Therefore, we suppose that the variation in the average Ti–O bond length d dominates the reduction of the Mott-Hubbard gap E_g under pressure. This can be quantified in terms of a gap deformation potential, $dE_g/d \ln d = 11(2)$ eV in the region of linear change.

Figure 6(b) evidences an unexpected nonlinear change of the optical gap with pressure: the initial slope of the absorption edge shift is only about half as large as compared to the region above 10 GPa. The increase in slope up to ~ 10 GPa can hardly be correlated with changes in the average bond length or the bond angles. This seems to indicate that the pressure-induced band gap closure depends not only on the bond lengths and angles, as is usually assumed, but also on the orbital state of the transition metal ion. Such view finds support in recent theoretical work [10], where under *isotropic compression* (that is, without orbital reorientation) the electronic gap closure is expected to occur only at ~ 100 GPa, i.e., at about twice the experimental estimate.

In summary, the pressure-induced structural changes in YTiO_3 were studied in detail by synchrotron x-ray diffraction. Distinct changes in the distortion of the TiO_6 octahedra around 10 GPa are attributed to a spatial reorientation of the occupied Ti $3d(t_{2g})$ orbitals. There is a structural similarity between YTiO_3 at 15 GPa and SmTiO_3 at ambient pressure, which suggests that YTiO_3 may lose its unusual property of being both ferromagnetic *and* insulating by turning antiferromagnetic under

compression. The combination of infrared transmission and x-ray diffraction experiments made it possible to obtain direct, quantitative information on the change of the electronic bandgap/bandwidth in a rare-earth transition metal perovskite together with a detailed knowledge of the associated structural changes. These results provide a framework for testing theoretical methods and models of the electronic structure of the t_{2g} -band titanates in the vicinity of the insulator-metal borderline.

We acknowledge stimulating discussion with O. K. Andersen, K. Held, and A. Yamasaki. We thank F. X. Zhang for support in the early stage of this study and M. Süpfle for technical support at ANKA.

* Corresponding author: E-mail I.Loa@fkf.mpg.de

- [1] H. Sawada and K. Terakura, *Phys. Rev. B* **58**, 6831 (1998).
- [2] T. Mizokawa and A. Fujimori, *Phys. Rev. B* **54**, 5368 (1996).
- [3] M. Itoh, M. Tsuchiya, H. Tanaka, and K. Motoya, *J. Phys. Soc. Jpn.* **68**, 2783 (1999).
- [4] J. Akimitsu *et al.*, *J. Phys. Soc. Jpn.* **12**, 3475 (2001).
- [5] H. Nakao *et al.*, *Phys. Rev. B* **66**, 184419 (2002).
- [6] F. Iga *et al.*, *Phys. Rev. Lett.* **93**, 257207 (2004).
- [7] T. Mizokawa, D. I. Khomskii, and G. A. Sawatzky, *Phys. Rev. B* **60**, 7309 (1999).
- [8] E. Pavarini *et al.*, *Phys. Rev. Lett.* **92**, 176403 (2004).
- [9] M. Mochizuki and M. Imada, *New J. Phys.* **6**, 154 (2004).
- [10] E. Pavarini, A. Yamasaki, J. Nuss, and O. K. Andersen, cond-mat/0504034.
- [11] C. Ulrich *et al.*, *Phys. Rev. Lett.* **89**, 167202 (2002).
- [12] G. Khaliullin and S. Okamoto, *Phys. Rev. Lett.* **89**, 167201 (2002).
- [13] D. A. MacLean, H.-N. Ng, and J. E. Greedan, *J. Solid State Chem.* **30**, 35 (1979).
- [14] M. Cwik *et al.*, *Phys. Rev. B* **68**, 060401 (2003).
- [15] A. Hammersley, computer program FIT2D, (ESRF, Grenoble, 1998).
- [16] A. C. Larson and R. B. von Dreele, GSAS: General Structure Analysis System. Report LAUR 86-748, Los Alamos National Laboratory, NM, USA, 1986.
- [17] B. H. Toby, *J. Appl. Cryst.* **34**, 210 (2001), computer program EXPGUI.
- [18] G. J. Piermarini, S. Block, J. D. Barnett, and R. A. Forman, *J. Appl. Phys.* **46**, 2774 (1975); H. K. Mao, J. Xu, and P. M. Bell, *J. Geophys. Res.* **91**, 4673 (1986).
- [19] I. Loa *et al.*, *Phys. Rev. Lett.* **87**, 125501 (2001).
- [20] M. Mochizuki and M. Imada, *J. Phys. Soc. Jpn.* **73**, 1833 (2004).
- [21] T. Katsufuji, Y. Taguchi, and Y. Tokura, *Phys. Rev. B* **56**, 10145 (1997).
- [22] T. Arima, Y. Tokura, and J. B. Torrance, *Phys. Rev. B* **48**, 17006 (1993).
- [23] Y. Okimoto *et al.*, *Phys. Rev. B* **51**, 9581 (1995).
- [24] D. A. Crandles, T. Timusk, J. D. Garret, and J. E. Greedan, *Physica C* **201**, 407 (1992).
- [25] M. Amboage, Ph.D. thesis, University of the Basque Country, Bilbao, Spain, 2003.